Geochemical Perspectives Letters

A secular increase in continental crust nitrogen during the Precambrian

B.W. Johnson[1,2*], C. Goldblatt[1]

OPEN ACCESS

doi: 10.7185/geochemlet.1731

Abstract

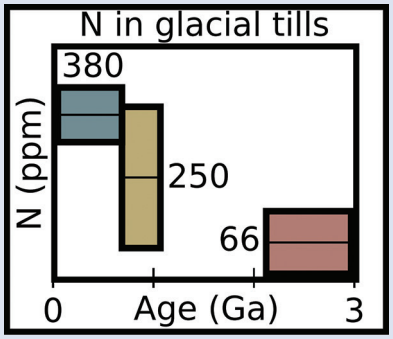

Recent work indicates the presence of substantial geologic nitrogen reservoirs in the mantle and continental crust. Importantly, this geologic nitrogen has exchanged between the atmosphere and the solid Earth over time. Changes in atmospheric nitrogen (*i.e.* atmospheric mass) have direct effects on climate and biological productivity. It is difficult to constrain, however, the evolution of the major nitrogen reservoirs through time. Here we show a secular increase in continental crust nitrogen through Earth history recorded in glacial tills (2.9 Ga to modern), which act as a proxy for average upper continental crust composition. Archean and earliest Palaeoproterozoic tills contain 66 ± 100 ppm nitrogen, whereas Neoproterozoic and Phanerozoic tills contain 290 ± 165 ppm nitrogen, whilst the isotopic composition has remained constant at ~4‰. Nitrogen has accumulated in the continental crust through time, likely sequestered from the atmosphere *via* biological fixation. Our findings support dynamic, non-steady state behaviour of nitrogen through time, and are consistent with net transfer of atmospheric N to geologic reservoirs over time.

Received 22 March 2017 | Accepted 26 July 2017 | Published 1 September 2017

Introduction

The evolution of the Earth System N cycle and the distribution of N in the Earth over the planet's history are not well constrained (Zerkle and Mikhail, 2017). Nitrogen moves between different reservoirs in the Earth system including the atmosphere, biosphere, and geosphere (Marty, 1995; Boyd, 2001; Busigny *et al.*, 2003, 2011). Changes in the distribution of N among the major reservoirs of the Earth (mantle, crust, and atmosphere) have direct effects on planetary habitability. Biologic productivity based on N-fixing can be limited under very low N_2 partial pressures (Klingler *et al.*, 1989), and the amount and speciation of N in the atmosphere affect temperature through direct or indirect greenhouse warming (Goldblatt *et al.*, 2009; Wordsworth and Pierrehumbert, 2013; Byrne and Goldblatt, 2015).

Higher N_2 atmospheres can enhance the effectiveness of greenhouse gases (Goldblatt *et al.*, 2009; Wordsworth and Pierrehumbert 2013), potentially providing a solution to the Faint Young Sun Paradox (Sagan and Mullen, 1972; Fuelner, 2012). Specifically, pressure-broadening (Goldblatt *et al.*, 2009) of CO_2 by an atmosphere with 2–3 fold more N_2 can provide warming consistent with constraints on atmospheric CO_2 content in the Archean (Sheldon, 2006). It is difficult to assess this, and other hypotheses of changing atmospheric mass (Som *et al.*, 2012, 2016; Barry and Hilton 2016), through direct measurements of palaeoatmospheric conditions. Another approach is to constrain the history of geologic N reservoirs.

One such reservoir is the continental crust. Current estimates for the amount of N in the modern continental crust range from 0.25 present atmospheric N mass (PAN, or 4×10^{18} kg N) (Rudnick and Gao, 2014) to 0.5 PAN (Goldblatt *et al.*, 2009; Johnson and Goldblatt, 2015). These estimates rely on measurements of individual rock types, which are then weighted by their proportion in the crust. For comparison, estimates of N in the Earth's interior range from 1 to 7 PAN in the Bulk Silicate Earth and >50 PAN in the core (Johnson and Goldblatt, 2015, and references therein). Modern subducted N is estimated to be 5×10^{-10} PAN *per* year (Johnson and Goldblatt, 2015) with non-arc outgassing of 1.75×10^{-11} PAN *per* year (Cartigny and Marty, 2013). The estimates of crustal N content may be biased, though, due to the effects of differential chemical weathering and alteration. In addition, these approaches offer no temporal resolution. As an alternative approach, we present measurements of glacial tills through time as a proxy for the upper continental crust.

Large glaciers and ice sheets erode a wide variety of rock types, and resulting glacial till will represent an average composition of the crust over which they erode. Thus, integration of many samples of glacial till can act as a proxy for average upper continental crust composition. This approach was first utilised by Goldschmidt (1933), but has since been used to estimate the upper continental crust composition of both Phanerozoic, juvenile crust (Canil and Lacourse, 2011) as well as the composition of the crust through time (Gaschnig *et al.*, 2016). Physical weathering and erosion by a glacier should

1. School of Earth and Ocean Sciences, University of Victoria, Victoria BC, Canada
2. Department of Geological Sciences, University of Colorado, Boulder, Boulder CO, USA
* Corresponding author (email: bwjohnso@uvic.ca)

not impart any isotopic fractionation on the samples. In addition, while weathering can produce locally distinct $\delta^{15}N$ values (Boyd, 2001), it is expected that large glaciers will represent an average composition, which will integrate local variation.

While biologic N cycling (Gruber and Galloway, 2008) has been a topic of research for well over a hundred years (Breneman, 1889), the geologic N cycle and exchange of N between the atmosphere and solid Earth have received far less attention. Some modelling efforts suggested near steady state N concentrations in the crust, mantle, and atmosphere over at least the Phanerozoic (Berner, 2006), and possibly for most of Earth history (Zhang and Zindler, 1993; Tolstikhin and Marty, 1998). In contrast, geochemistry (Mitchell *et al*., 2010; Busigny *et al*., 2011; Barry and Hilton, 2016), other models (Hart, 1978; Stüeken *et al*., 2016), and physical proxies (Som *et al*., 2012, 2016; Kavanagh and Goldblatt, 2015) directly contradict the steady state hypothesis. The later proxies are consistent with movement of N between different reservoirs of the Earth and significant changes in the mass of the atmosphere over time. Additional thermodynamic calculations argue that the evolution of mantle redox and Eh-pH state at subduction zones directly affects N_2 outgassing, and therefore the distribution of N in the Earth through time (Mikhail and Sverjensky, 2014).

Either the distribution of N among the main reservoirs of the Earth (atmosphere, mantle, continental crust) has been in steady state over Earth history or it has been more dynamic. A difficulty in assessing the validity of steady state and dynamic interpretations of N distribution over Earth history is reconstructing N concentrations in geologic reservoirs in the past. The analysis of glacial tills presented herein suggests an increase in continental N through time, providing a temporal constraint on one of the three major N reservoirs of the Earth system.

Nitrogen in Glacial Tills

We analysed a series of tills from Gaschnig *et al*. (2016) for N concentration and N isotopes. These till samples consisted of predominantly fine grained matrix material, and come from formations as old as 2.9 Ga to formations as young as 0.3 Ga. We have also included a younger till, Till-4, which is a standard provided by the Geological Survey of Canada.

Nitrogen concentrations are low in glacial tills during the Archean and earliest Palaeoproterozoic, moderate and variable during the Neoproterozoic, and moderate-high and less variable during the Phanerozoic (Fig. 1, Table 1, Supplementary Information). We define "low" as less than average granite, 54 ppm (Johnson and Goldblatt, 2015), "high" as approaching average upper crust sedimentary rocks, >400 ppm, and "moderate" as in between. Performing Student's t-test (Student, 1908) indicates that both the mean, shown with one standard deviation, Neoproterozoic (250 ± 180 ppm) and Phanerozoic (380 ± 50 ppm) concentrations are significantly different from the mean of the Archean and earliest Palaeoproterozoic (66 ± 100 ppm) samples. There appears to be a secular increase in N content in the continental crust through time.

Table 1 Proportion of till samples in each age group that have high (>400 ppm), low (<54 ppm), and moderate (in between) N.

Age	% low	% moderate	% high
Archean	100	0	0
Palaeoproterozoic	75	25	0
Neoproterozoic	10	60	30
Phanerozoic	0	50	50

In contrast, mean (plus one standard deviation) $\delta^{15}N$ values remain constant within error for all samples, with a value of 3.5 ± 1.4 ‰ for the Archean and earliest Palaeoproterozoic, 4.9 ± 4.0 ‰ for Neoproterozoic, and 4.9 ± 2.6 ‰ for the Phanerozoic (Fig. 2). These three populations are not significantly different using Student's t-test. Such isotopic consistency implies either no biologic fractionation during weathering or consistent biologic involvement in glacial weathering through time.

The increase in N concentration through time does not appear to be the result of progressive alteration. There is no correlation between N concentration and $\delta^{15}N$, the chemical index of alteration (CIA), or Cs/Zr (see Supplementary information). If N was being lost due to weathering or volatilisation, low N samples should have high $\delta^{15}N$ and CIA values. If N were behaving as a fluid-mobile element like Cs, there would be a correlation between N and Cs/Zr, with Zr being a non-fluid mobile element. Such lack of correlation indicates that changes in N concentration are not explained by progressive alteration through time.

Two of the low N samples from the Neoproterozoic may not be fully representative of general, contemporaneously formed, upper crust. One result is from erosion of 1.1 Ga Grenville-associated units (Konnarock Formation) and a second is heavily influenced by erosion of bimodal volcanism (Pocatello Formation) (Gaschnig *et al*., 2016). We suggest Grenvillian rocks may not be representative of the average upper crust, as they typically expose deeper crust from within an orogenic belt. Clasts in the Konnarock Formation are primarily middle to lower crustal granites (Rankin, 1993). Globally, granites average 54 ppm N (Johnson and Goldblatt, 2015), much lower than sedimentary or metasedimentary rocks. Though more sparsely measured, volcanic rocks tend to have low N as well, around 0.1 to 10 ppm (Johnson and Goldblatt, 2015), owing to the high volatility of N during the eruption of oxidised magma (Libourel *et al*., 2003). Tills that sample only igneous rocks may be biased towards low N.

Additionally, while there is a correlation between N concentration and Rb and K for low N samples, there is not for moderate and high N samples (Supplementary Information). Nitrogen is commonly found as NH_4^+ in geologic samples and substitutes for K in silicates (Honma and Itihara, 1981; Hall, 1999). Many studies have observed correlation between N, K, and Rb in metasediments (Bebout and Fogel, 1992; Busigny *et al*., 2003). Thus, low N samples suggest incorporation of metasedimentary N into the crust *via* recycling of N into the mantle at subduction zones (Marty 1995; Goldblatt *et al*., 2009; Busigny *et al*., 2011; Mikhail and Sverjensky, 2014; Barry and Hilton, 2016). Higher N samples imply an additional, or more efficient, transfer mechanism.

There appears to be a relationship between the present continent of the sample outcrop and N concentrations (Fig. 1). African samples appear to increase in the Palaeoproterozoic and remain high during the Neoproterozoic and Phanerozoic. In contrast, samples from North America are low-moderate into the Neoproterozoic with the most recent sample showing high N concentrations. The single sample from South America and both samples from Asia have moderate to high N. While the strongest control on N concentration appears to be age, it is possible that different continents have a different N history due to differences in their growth history (Supplementary Information). It is also possible that this apparent relationship between present-day geography and N concentration is simply an artefact of a small number of samples.

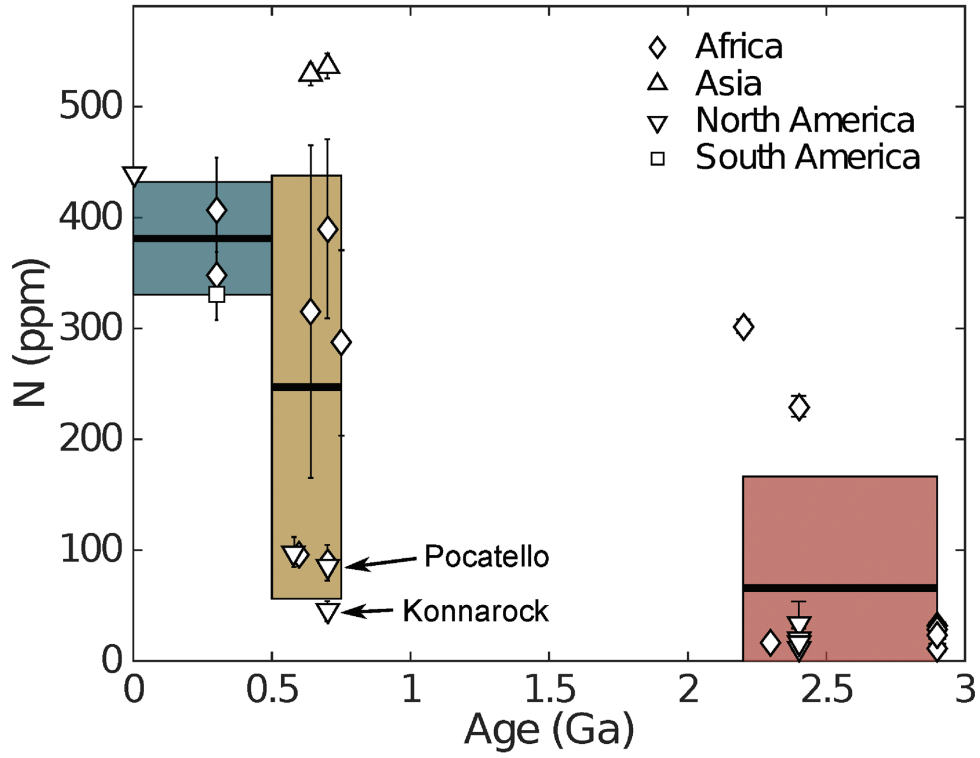

Figure 1 Nitrogen concentration in glacial tills through time. Means of triplicate analyses of each sample, with standard deviation, are shown with shapes representing modern continent of exposure. Black lines and coloured boxes show mean and standard deviation of Archean-Palaeoproterozoic, Neoproterozoic, and Phanerozoic samples. Low N samples from units that have eroded primarily igneous terranes in North America are noted, and discussed in the text.

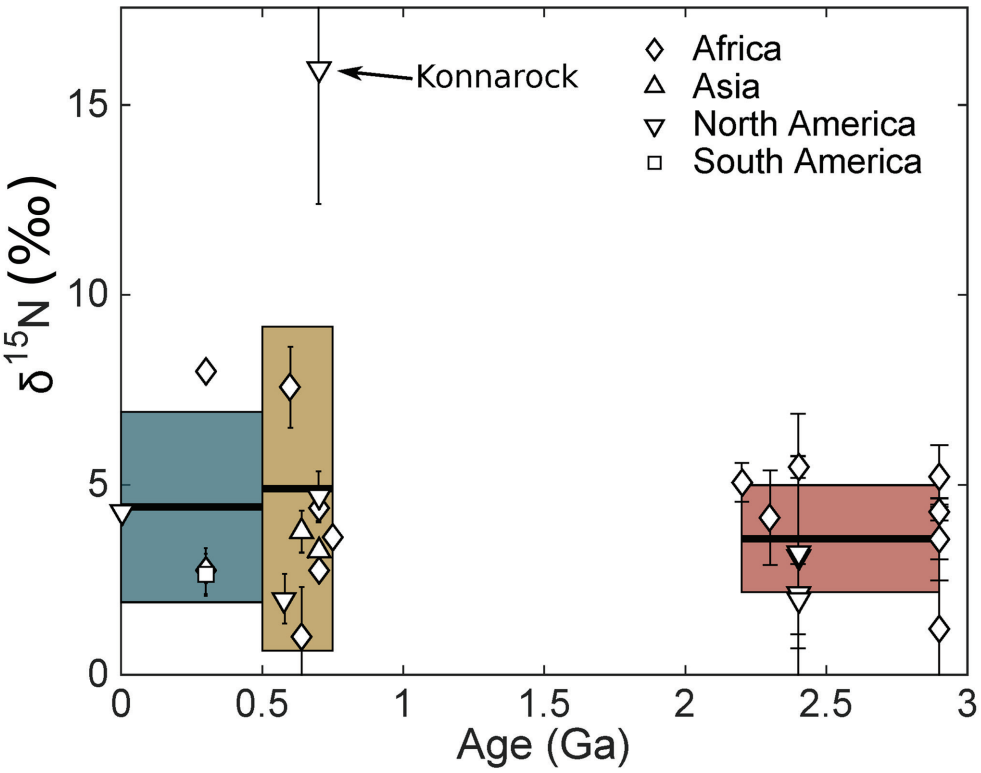

Figure 2 Nitrogen isotope values (‰) in glacial tills through time. Averages (black lines) for each time period (Archean-Palaeoproterozoic, Neoproterozoic, and Phanerozoic) are equivalent within error (one standard deviation, coloured boxes), indicating no change in the isotopic character of the continental crust through time.

Implications for Atmospheric Evolution

How, then, did N accumulate? The isotopic signature is consistent through the record, and is most similar to either modern average marine NO_3^- or sedimentary N (+5 to +7 ‰). The till record is distinct from both the modern atmosphere (0 ‰) and the best estimate for the MORB-source mantle value of -5 ‰, (Marty, 1995). The parsimonious explanation would be incorporation of biologically processed N into the crust with time. Such processing implies N-fixing, thus this N is ultimately of atmospheric origin.

The mechanisms which transfer N into the continental crust through time are speculative, but have important implications for models of N distribution through time. The most concentrated reservoirs of continental N are in sedimentary and metasedimentary rocks (concentrations 400–500 ppm), with concentrations much higher than igneous rocks (*e.g.*, 54 ppm in granites, 0.1–10s ppm in basalts; Johnson and Goldblatt, 2015). One likely mechanism of transfer, then, is burial of biologically-processed N at continental margins followed by accretion. An additional mechanism could be input of N at subduction zones. Sparse N concentration and isotopic data suggests that granitic N content has increased through time (Supplementary Information). In addition, granitic samples show an increase in $\delta^{15}N$ values through time, consistent with enhanced incorporation of biologically processed N.

The exact timing of incorporation of N is also difficult to determine. There are no glacial deposits from the Mesoproterozoic, rendering this till-based approach ill-suited to this time period. Interestingly, there are two high-N (>200 ppm) samples from the Palaeoproterozoic. Gaschnig *et al*. (2016) note a distinct change in the composition of tills between the Archean and Palaeoproterozoic glaciations, reflecting a transition from greenstone/komatiite dominated Archean crust to more felsic crust in the Proterozoic. This trend is perhaps mirrored in some of the N analyses, with more felsic crust having higher N concentration.

Regardless of the timing of the increase of crustal N, we can compare the upper crust N budget from the till proxy to previous work. Johnson and Goldblatt (2015) suggest 150 ± 22 ppm N in the upper crust, while Rudnick and Gao (2014) suggest 83 ppm. We use a total continental crust mass of 2.28×10^{22} kg (Laske *et al*., 2013), with the upper crust being 53 % of the total (Wedepohl, 1995). The Rudnick and Gao (2014) estimate of 83 ppm N yields 0.1×10^{18} kg N (0.25 PAN) in the upper crust and 150 ppm from Johnson and Goldblatt (2015) suggests 0.5 PAN. Based on exposed and buried outcrop area, the upper continental crust is 28 % Phanerozoic, 31 % Neoproterozoic, 16 % Mesoproterozoic, 15 % Palaeoproterozoic, and 10 % Archean (Goodwin, 1991, 1996). Given this crust distribution, and assuming the Mesoproterozoic has the same N concentration as the Archean/Palaeoproterozoic, our work suggests an upper crust N concentration of 210 ppm, equivalent to 2.5×10^{18} kg N, or 0.63 PAN (Table 2).

Importantly, the N content of the lower crust is poorly constrained, but could be a significant N reservoir as well. Johnson and Goldblatt (2015) suggest 17 ppm N in the lower crust, which would result in a total continental crust N concentration of 120 ppm and a N mass of 2.7×10^{18} kg.

The trend of increased N concentration in the continental crust over time is consistent with non-steady state behaviour of N through Earth history. Specifically, the till record is consistent with net atmospheric drawdown through time (Goldblatt *et al*., 2009; Busigny *et al*., 2011; Barry and Hilton, 2016). While the tills provide a constraint on the evolution of one of the three major N reservoirs (continental crust), determining the exact evolution of the other two (mantle and atmosphere) requires more analyses. We cannot necessarily rule out modern or lower pN_2 at specific points in Earth history (*e.g.*, Som *et al*., 2012, 2016; Marty *et al*., 2013) but the till data is most consistent with higher atmospheric mass in the past. The balance of mantle outgassing at mid-ocean ridges and arcs to in-gassing at subduction zones is an important, and unconstrained, parameter, over Earth history. Strong net mantle outgassing would be required to have non-decreasing atmospheric N through time.

Table 2 Distribution of upper continental crust ages after Goodwin (1991, 1996). We assume that tills accurately sample crust of each age, and that the Mesoproterozoic has the same N concentration as the Archean/Palaeoproterozoic.

Age	% crust	N (ppm)
Phanerozoic	28	380
Neoproterozoic	31	250
Mesoproterozoic	16	66
Palaeoproterozoic	15	66
Archean	10	66
	Total upper crust [N] = 210 ppm mass = 2.5×10^{18} kg N	

Acknowledgements

The authors thank Richard Gaschnig and Roberta Rudnick for providing glacial till samples as well as Dante Canil for the initial suggestion to use glacial tills as a crust composition proxy. We also thank Natasha Drage at the University of Victoria for assistance with sample compilation. Andy Schauer at the University of Washington assisted in isotopic analyses. Funding was provided in an NSERC Discovery Grant to CG. We thank Sami Mikhail and an anonymous reviewer for constructive feedback, as well as Helen Williams for editorial support.

Editor: Helen Williams

Additional Information

Supplementary Information accompanies this letter at www.geochemicalperspectivesletters.org/article1731

Reprints and permission information are available online at http://www. geochemicalperspectivesletters.org/copyright-and-permissions

Cite this letter as: Johnson, B.W., Goldblatt, C. (2017) A secular increase in continental crust nitrogen during the Precambrian. *Geochem. Persp. Let.* 4, 24–28.

References

Barry, P., Hilton, D. (2016) Release of subducted sedimentary nitrogen throughout Earth's mantle. *Geochemical Perspectives Letters* 2, 148–159.

Bebout, G., Fogel, M. (1992) Nitrogen-isotope compositions of metasedimentary rocks in the Catalina Schist, California: implications for metamorphic devolatilization history. *Geochimica et Cosmochimica Acta* 56, 2839–2849.

Berner, R.A. (2006) Geological nitrogen cycle and atmospheric N_2 over phanerozoic time. *Geology* 34, 413–415.

Boyd, S. (2001) Nitrogen in future biosphere studies. *Chemical Geology* 176, 1–30.

Breneman, A. (1889) The Fixation of Atmospheric Nitrogen. (Concluded from Issue 1). *Journal of the American Chemical Society* 11, 31–48.

Busigny, V., Cartigny, P., Philippot, P., Ader, M., Javoy, M. (2003) Massive recycling of nitrogen and other fluid-mobile elements (K, Rb, Cs, H) in a cold slab environment: evidence from HP to UHP oceanic metasediments of the Schistes Lustrés nappe (western Alps, Europe). *Earth and Planetary Science Letters* 215, 27–42.

Busigny, V., Cartigny, P., Philippot, P. (2011) Nitrogen isotopes in ophiolitic metagabbros: A re-evaluation of modern nitrogen fluxes in subduction zones and implication for the early earth atmosphere. *Geochimica et Cosmochimica Acta* 75, 7502–7521.

Byrne, B., Goldblatt, C. (2015) Diminished greenhouse warming from Archean methane due to solar absorption lines. *Climate of the Past* 11, 559–570.

Canil, D., Lacourse, T. (2011) An estimate for the bulk composition of juvenile upper continental crust derived from glacial till in the North American Cordillera. *Chemical Geology* 284, 229–239.

Cartigny, P., Marty, B. (2013) Nitrogen isotopes and mantle geodynamics: The emergence of life and the atmosphere-crust-mantle connection. *Elements* 9, 359–366.

Fuelner, G. (2012) The faint young sun problem. *Reviews of Geophysics* 50, 1–29.

Gaschnig, R.M., Rudnick, R.L., McDonough, W.F., Kaufman, A.J., Valley, J.W., Hu, Z., Gao, S., Beck, M.L. (2016) Compositional evolution of the upper continental crust through time, as constrained by ancient glacial diamictites. *Geochimica et Cosmochimica Acta* 186, 316–343.

Goldblatt, C., Claire, M., Lenton, T., Matthews, A., Watson, A., Zahnle, K. (2009) Nitrogen- enhanced greenhouse warming on early Earth. *Nature Geoscience* 2, 891–896.

Goldschmidt, V. (1933) Grundlagen der quantitativen Geochemie. *Fortschrift Mineralogie* 17, 12.

Goodwin, A.M. (1991) *Precambrian Geology: the Dynamic Evolution of the Continental Crust*. Academic Press, London.

Goodwin, A.M. (1996) *Principles of Precambrian geology*. Academic Press, London.

Gruber, N., Galloway, J. (2008) An Earth-system perspective of the global nitrogen cycle. *Nature* 451, 293–296.

Hall, A. (1999) Ammonium in granites and its petrogenetic significance. *Earth-Science Reviews* 45, 145–165.

Hart, M.H. (1978) The evolution of the atmosphere of the earth. *Icarus* 33, 23–39.

Honma, H., Itihara, Y. (1981) Distribution of ammonium in minerals of metamorphic and granitic rocks. *Geochimica et Cosmochimica Acta* 45, 983–988.

Johnson, B.W., Goldblatt, C. (2015) The Nitrogen Budget of Earth. *Earth Science Reviews* 148, 150–173.

Kavanagh, L., Goldblatt, C. (2015) Using raindrops to constrain past atmospheric density. *Earth and Planetary Science Letters* 413, 51–58.

Klingler, J., Mancinelli, R., White, M. (1989) Biological nitrogen fixation under primordial martian partial pressures of dinitrogen. *Advances in Space Research* 9, 173–176.

Laske, G., Masters, G., Ma, Z., Pasyanos, M. (2013) Update on CRUST1.0 - A 1-degree Global Model of Earth's Crust. *Geophysical Research Abstracts* 15, Abstract EGU2013-2658.

Libourel, G., Marty, B., Humbert, F. (2003) Nitrogen solubility in basaltic melt. Part I. Effect of oxygen fugacity. *Geochimica et Cosmochimica Acta* 67, 4123–4135.

Marty, B. (1995) Nitrogen content of the mantle inferred from N_2–Ar correlation in oceanic basalts. *Nature* 377, 326–329.

Marty, B., Zimmermann, L., Pujol, M., Burgess, R., Philippot, P. (2013) Nitrogen isotopic composition and density of the Archean atmosphere. *Science* 342, 101–104.

Mikhail, S., Sverjensky, D.A. (2014) Nitrogen speciation in upper mantle fluids and the origin of Earth's nitrogen-rich atmosphere. *Nature Geoscience* 7, 816–819.

Mitchell, E.C., Fischer, T.P., Hilton, D.R., Hauri, E.H., Shaw, A.M., de Moor, J.M., Sharp, Z.D., Kazahaya, K. (2010) Nitrogen sources and recycling at subduction zones: Insights from the Izu-Bonin-Mariana arc. *Geochemistry, Geophysics, Geosystems* 11, Q02X11, doi:10.1029/2009GC002783.

Rankin, D.W. (1993) The volcanogenic Mount Rogers Formation and the overlying glaciogenic Konnarock Formation; two late Proterozoic units in southwestern Virginia. Technical report, USGPO; US Geological Survey, Map Distribution.

Rudnick, R., Gao, S. (2014) Composition of the Continental Crust. *Treatise on Geochemistry* 4, 1–69.

Sagan, C., Mullen, G. (1972) Earth and Mars: Evolution of atmospheres and surface temperatures. *Science* 177, 52–56.

Sheldon, N.D. (2006) Precambrian paleosols and atmospheric CO2 levels. *Precambrian Research* 147, 148–155.

Som, S.M., Catling, D.C., Harnmeijer, J.P., Polivka, P.M., Buick, R. (2012) Air density 2.7 billion years ago limited to less than twice modern levels by fossil raindrop imprints. *Nature* 484, 359–362.

Som, S.M., Buick, R., Hagadorn, J.W., Blake, T.S., Perreault, J.M., Harnmeijer, J.P., Catling, D.C. (2016) Earth's air pressure 2.7 billion years ago constrained to less than half of modern levels. *Nature Geoscience* 9, 448–451.

Student (1908) The probable error of a mean. *Biometrika* 6, 1–25.

Stüeken, E., Kipp, M., Koehler, M., Schwieterman, E., Johnson, B.W., Buick, R. (2016) Modeling pN2 through geologic time: Implications for atmospheric biosignatures. *Astrobiology* 16, 949–963.

Tolstikhin, I., Marty, B. (1998) The evolution of terrestrial volatiles: a view from helium, neon, argon and nitrogen isotope modelling. *Chemical Geology* 147, 27–52.

Wedepohl, H.K. (1995) The composition of the continental crust. *Geochimica et Cosmochimica Acta* 59, 1217–1232.

Wordsworth, R., Pierrehumbert, R. (2013) Hydrogen-nitrogen greenhouse warming in earth's early atmosphere. *Science* 339, 64–67.

Zerkle, A., Mikhail, S. (2017) The geobiological nitrogen cycle: From microbes to the mantle. *Geobiology* 15, 343–352.

Zhang, Y., Zindler, A. (1993) Distribution and evolution of carbon and nitrogen in Earth. *Earth and Planetary Science Letters* 117, 331–345.

Geochemical Perspectives Letters

A secular increase in continental crust nitrogen during the Precambrian

B.W. Johnson[1,2*], C. Goldblatt[1]

Supplementary Information

The Supplementary Information includes:

- Sample Description and Collection
- Detailed N Analytical Methods
- Constraining Post-depositional Alteration
- Mineral Hosts for Nitrogen
- Nitrogen Concentrations by Continent
- Granitic Nitrogen
- Table S-1
- Figures S-1 to S-7
- Supplementary Information References

Sample Description and Collection

All samples analysed were collected by Gaschnig *et al.* (2016). These samples were collected specifically to assess changes in the composition of the upper continental crust through time. Large ice sheets typically erode a wide variety of rock types, thus till samples should represent an average upper crustal composition. The following is a summary of their collection and sample preparation techniques, but please see the original paper for more detail.

The sampling strategy focused on collecting fine grained material. This was achieved by collecting massive diamictite and some drop-stone bearing argillite. In both cases, the fine grained matrix was crushed in an alumina jaw crusher, clasts larger than 5 mm were removed, and the remaining sample crushed to a fine powder using an alumina swing mill. Excepting the Palaeoproterozoic Pecors, Neoproterozoic Blasskranz, and Ordovician Pakhuis formations, all samples are given as composites of each stratigraphic unit. That is, individual crushed samples were homogenised to give a representative average mixture for each formation.

Gaschnig *et al.* (2016) determined major element compositions using X-ray fluorescence and trace element composition using laser-ablation ICP-MS techniques. We use their values directly, including chemical index of alteration (CIA), which is calculated as $Al_2O_3/(Al_2O_3 + CaO + K_2O + Na_2O)$. Note that they corrected CaO to remove any influence of carbonates and apatite.

Detailed N Analytical Methods

All N measurements were done at the University of Washington's IsoLab, following the procedure outlined in Stüeken (2013). Briefly, between 10–100 mg of sample powder were weighed into a 9 x 5 mm Sn capsule. Samples and standards were analysed on a Thermo-Finnigan MAT 253 coupled to a Costech Elemental Analyzer. Standards used were two glutamic acids (GA-1, GA-2), and two internal standards (dried salmon and organic-rich McRae shale). Samples were flash-combusted at 1000 ˚C in a combustion column packed with cobaltous oxide (combustion aid) and silvered cobaltous oxide (sulphur scrubber). Combustion products passed over a reduced copper column at 650 ˚C to convert all N to N_2 and absorb excess O_2. Lastly, sample gas passed through a magnesium perchlorate trap to absorb water and a 3 m gas chromatography column to separate N_2 from O_2. All analyses were quantified using IsoDat software.

Errors reported for individual samples are one standard deviation based on triplicate analysis of each sample. The mean and one standard deviation are shown for each age group (Archean/Palaeoproterozoic, Neoproterozoic, Phanerozoic) are simply calculated from all samples that fall within each age window. Lower N concentrations generally result in greater uncertainty in isotopic measurements due to smaller amounts of N released during analysis. Thus, isotopic uncertainties for the low N samples, most of the Archean/Palaeoproterozoic and some Neoproterozoic, are generally higher (Table S-1). In addition, some error may have been introduced due to not preparing samples in a vacuum. It is possible that some atmospheric N_2 adhered to the powder, though any contamination is suspected to be small due to distinctly non-zero (*i.e.* non-atmospheric) $\delta^{15}N$ values and lack of correlation between N concentration and $\delta^{15}N$. If atmospheric contamination was a major issue, we would expect samples with high N to have low $\delta^{15}N$ values, which is not observed. This interpretation implies that $\delta^{15}N$ values in tills are non-zero initially, which is consistent with observed $\delta^{15}N$ values from a wider variety of continental rocks (Johnson and Goldblatt, 2015).

1. School of Earth and Ocean Sciences, University of Victoria, Victoria BC, Canada
2. Department of Geological Sciences, University of Colorado, Boulder, Boulder CO, USA
* Corresponding author (email: bwjohnso@uvic.ca)

Table S-1 Nitrogen concentration and stable isotopic data. Samples analysed are from Gaschnig *et al.* (2016) and sample names herein are those used in the original publication. Age is in Ga, N concentration is in ppm and $\delta^{15}N$ is in per mille. Non-N data is from Gaschnig *et al.* (2016) with SiO_2 and K_2O in wt. % with all others in ppm. CIA is $Al_2O_3/(Al_2O_3 + CaO + K_2O + Na_2O)$ corrected to remove carbonate and apatite CaO. Continent indicates continent where sample was collected. AF – Africa, NA – North America, AS – Asia, SA – South America.

Stratigraphic unit	Continent	Age	N	$\delta^{15}N$	SiO_2	Al_2O_3	CaO	Na_2O	K_2O	CIA	Rb	Zr	Cs
Mozaan Group	AF	2.9	24	4.3	58.8	8.95	0.38	0.78	1.67	71	49.7	93.1	
Mozaan Group	AF	2.9	31	5.6	58.1	8.75	0.52	0.63	1.42	72	35.1	84.9	1.32
Mozaan Group	AF	2.9	28	5.8	58.9	8.94	0.13	0.08	0.96	88	33.4	103	2.53
Mozaan Group	AF	2.9			59.3	9.07	0.14	0.72	1.78	74	75.8	166	4.09
Mozaan Group	AF	2.9			54	9.52	0.76	0.66	1.51	72	37.7	89.2	1.38
Mozaan Group	AF	2.9			57.6	8.51	1.25	0.56	1.69	70	37.4	89	1.18
Mozaan Group	AF	2.9			55.9	7.82	0.16	0.51	0.8	81	17.3	66.3	0.9431
Afrikander Frm	AF	2.9	9	3.1	64	8.49	5.94	0.5	0.41	80	9.2	92.7	0.3083
Afrikander Frm	AF	2.9	11	2.8	64.1	8.24	6.09	0.38	0.49	82			
Afrikander Frm	AF	2.9	16	4.8	63.9	8.32	5.99	0.42	0.34	83	8.14	50.3	0.31
Afrikander Frm	AF	2.9			62.1	8.53	5.87	0.9	1.07	67			
Promise Formation West Rand Group Witwatersrand	AF	2.9	22	4.2	61	15.5	0.54	0.54	2.43	78	97.7	159	5.01
Promise Formation West Rand Group Witwatersrand	AF	2.9	21	4.1	85.6	7.18	1.25	0.93	1.48	60	57.2	44.1	3.34
Promise Formation West Rand Group Witwatersrand	AF	2.9	28	4.5	63.4	11.1	0.66	0.44	0.59	84	25.5	120	1.26
Coronation Formation West Rand Group Witwatersrand	AF	2.9	33	2	74.3	15.1	0.21	0.35	3.29	78	124	192	9.07
Coronation Formation West Rand Group Witwatersrand	AF	2.9	35	2.5	72.3	15.1	0.46	0.33	3	78	110	181	8.77
Coronation Formation West Rand Group Witwatersrand	AF	2.9	30	-0.9	68.8	15.7	0.47	0.38	2.72	80	97.6	191	7.14
Coronation Formation West Rand Group Witwatersrand	AF	2.9			72.2	15.7	0.7	0.3	2.57	81	93.7	213	7.32
Coronation Formation West Rand Group Witwatersrand	AF	2.9			71.7	13.9	0.14	0.23	2.65	80			
Bottle Creek Formation	NA	2.4	10	2.8	72.2	13.1	0.61	4.39	1.82	57	66	130	1.84
Bottle Creek Formation	NA	2.4	42	0.9	70.6	13.4	0.49	3.92	2	59	68	200	1.73
Bottle Creek Formation	NA	2.4	48	2.7	71.7	13.2	0.52	3.97	1.89	59	56	215	1.66
Bottle Creek Formation	NA	2.4			70.9	13.5	0.46	4.1	1.76	59	55	209	1.23
Gowganda Formation	NA	2.4	11	3.4	69.3	13.8	0.34	5.08	1.4	57	50.7	85.4	1.27
Gowganda Formation	NA	2.4	10	0.5	70.5	13.8	0.26	4.13	2.21	59	91.1	256	2.43
Gowganda Formation	NA	2.4	13	2.1									
Bruce Formation	NA	2.4	19	-0.9	71.3	14.1	0.35	4.23	2.9	57	96.5	153	0.925
Bruce Formation	NA	2.4	12	3.6	62.3	17.4	0.41	3.6	3.84	62	159	197	1.89
Bruce Formation	NA	2.4	30	6.6	70.5	13	0.32	3.51	1.46	63	68.7	141	1.38
Ramsay Lake Formation	NA	2.4	14	3.1	61.2	15.8	0.53	2.31	1.86	71	71	163	2.31
Ramsay Lake Formation	NA	2.4	20	3.6	62.6	12.9	2.51	1.43	1.38	68	68.1	143	2.4
Ramsay Lake Formation	NA	2.4	14	3	59.2	15	0.71	1.41	1.55	76	77.3	154	2.35
Gowganda Formation	NA	2.4	11	3.4	65.5	14.9	0.45	4.52	2.07	59	66.7	138	1.07
Gowganda Formation	NA	2.4	10	0.5	65.3	15.1	0.48	4.8	2.17	58	76.2	161	1.22
Gowganda Formation	NA	2.4	13	2.1	70.2	13.6	0.37	4.96	2.06	56	48.1	152	0.608
Gowganda Formation	NA	2.4			66.7	14.2	0.27	4.64	1.66	59	60.1	148	0.803
Gowganda Formation	NA	2.4			65.2	15.2	1.16	5.62	2.27	53	67	154	1.12
Gowganda Formation	NA	2.4			64.7	15.3	1.15	5.67	2.39	53	72.4	148	1.08
Gowganda Formation	NA	2.4			71.8	13.5	0.72	4.98	3.14	52	95.6	137	1.43
Gowganda Formation	NA	2.4			65.2	14.7	0.71	4.75	2.2	57	57.7	128	
Gowganda Formation	NA	2.4			66.7	14.5	0.68	5.34	0.91	58	33.7	131	0.767
Gowganda Formation	NA	2.4			74.1	11	1.13	2.52	3.83	52			
Gowganda Formation	NA	2.4			66.7	12.6	3.16	3.9	1.24	49	35.3	94.8	0.455
Gowganda Formation	NA	2.4			66.9	12.5	2.14	2.31	1.56	58	37.6	129	1.25
Makganyene Formation	AF	2.3	15	4.9	50.9	7.04	6.5	0.06	0.54	92	17.1	101	2
Makganyene Formation	AF	2.3	15	4.8	53.3	8.18	5.37	0.08	0.74	91	22.5	109	2.12
Makganyene Formation Transvaal/Griqualand	AF	2.3	18	2.7	53.2	5.96	6.11	0.03	0.2	98	7.19	93.4	1.59
Makganyene Formation Transvaal/Griqualand	AF	2.3			60.3	10.6	0.59	0.05	1.27	89	36	106	2.08
Makganyene Formation	AF	2.3			61	8.81	1.69	0.03	1.45	86	54.8	105	1.54
Makganyene Formation	AF	2.3			61.4	9.04	2.07	0.04	1.81	83	46	121	1.54
Timeball Hill Formation	AF	2.2	295	5.2	61.8	19.6	0.83	0.22	5.43	75	266	202	18.3

Table S-1 Cont.

Stratigraphic unit	Continent	Age	N	$\delta^{15}N$	SiO_2	Al_2O_3	CaO	Na_2O	K_2O	CIA	Rb	Zr	Cs
Timeball Hill Formation	AF	2.2	306	4.5	63.8	16	0.91	1.07	3.26	71	173	180	13.6
Timeball Hill Formation	AF	2.2	305	5.5	63.4	15.9	0.97	1.24	3.1	70	168	149	13.2
Timeball Hill Formation	AF	2.2			71	11	3.33	3.21	0.91	48	49.3	86.2	3.72
Timeball Hill Formation	AF	2.2			64.1	15.1	2.42	1.38	3.01	66	158	159	12.6
Timeball Hill Formation	AF	2.2			64.5	15.5	1.45	1.27	3.09	68	170	148	13.7
Duitschland Formation	AF	2.4	230	5.8	56.8	24.5	0.23	0.14	6.14	78	198	224	17
Duitschland Formation	AF	2.4	239	5.3	55.1	23.3	0.25	0.15	5.38	79	183	297	15.1
Duitschland Formation	AF	2.4	220	5.3	63.1	10.9	1.4	0.06	1.9	84	69.9	113	4.01
Duitschland Formation	AF	2.4			63.9	11	2.15	0.05	1.88	85	72.4	129	4.08
Duitschland Formation	AF	2.4			31.7	7.57	10.42	0.05	0.79	91	28.8	71.9	1.79
Konnarock Formation	NA	0.7	54	12.2	64.7	15	0.65	2.07	5.45	60	220	352	5.66
Konnarock Formation	NA	0.7	36	19.3	68.1	14.2	0.52	2.22	5.22	59	202	392	5.3
Konnarock Formation	NA	0.7	45	16.4	68.2	14.2	0.68	3.06	4.26	58	162	334	2.57
Konnarock Formation	NA	0.7			68	13.6	1.44	3.09	3.64	55	139	300	2.43
Konnarock Formation	NA	0.7			67.6	13.8	1.62	3.1	3.69	54	140	331	2.44
Konnarock Formation	NA	0.7			67.7	13.8	1.6	3.1	3.73	54	136	336	2.31
Konnarock Formation	NA	0.7			68.9	13.9	1.56	2.75	4.39	54	154	387	3.78
Konnarock Formation	NA	0.7			69.1	13.9	1.77	2.85	4.58	53	153	360	3.51
Gucheng Formation near bottom of unit	AS	0.7	524	3.3	66.5	14.4	1.37	1.24	3.55	65	99.1	172	3.64
Gucheng Formation	AS	0.7	545	3.4	65.6	14.1	2.11	1.37	3.17	64	91	194	3.36
Gucheng Formation	AS	0.7	542	3.1	68	14.1	0.99	1.25	3.22	67	90.8	197	3.22
Gucheng Formation top of unit	AS	0.7			66.2	15	0.47	0.63	3.63	73	101	205	3.88
Gucheng Formation	AS	0.7			67.9	13.7	0.42	0.58	3.36	73	90.8	208	3.97
Nantuo Formation lower part of unit	AS	0.64	539	4.3	66.7	14.8	1.08	1.31	3.53	66	96.6	187	3.97
Nantuo Formation middle part of unit	AS	0.64	519	3.2	66	14.7	1.39	1.25	3.62	65	102	213	4.24
Nantuo Formation top of unit	AS	0.64	530	3.8	67.3	14.5	1.57	1.19	3.76	65	105	238	4.46
Nantuo Formation	AS	0.64			58.7	16.3	2.31	2.27	3.1	60	94	159	3.81
Nantuo Formation	AS	0.64			64.6	13.8	2.6	0.97	3.29	68	100	216	5.31
Nantuo Formation	AS	0.64			66.1	13.2	1.79	0.96	2.94	68	90.3	211	4.71
Nantuo Formation	AS	0.64			66.2	13.4	1.78	0.81	3.12	69	94.1	205	4.83
Nantuo Formation	AS	0.64			66.6	13.8	1.68	0.85	3.38	69	98.9	179	5.04
Nantuo Formation	AS	0.64			64.5	14.6	2	1.67	3.32	62	108	184	4.81
Nantuo Formation	AS	0.64			65.1	14.6	2.18	1.44	3.43	64	93.9	190	3.92
Nantuo Formation	AS	0.64			64.9	14.2	1.97	0.99	3.63	67	103	193	4.4
Nantuo Formation	AS	0.64			63.8	14.4	2.4	0.81	3.8	69	107	188	4.71
Nantuo Formation	AS	0.64			64.9	14.2	2.46	0.8	3.76	68	106	199	4.48
Pocatello Formation upper diamictite	NA	0.7	99	4.6	71.1	11.8	1.71	0.31	3.89	71	132	388	4.23
Pocatello Formation upper diamictite	NA	0.7	78	4.1	70.7	12.7	0.49	0.73	3.95	68	136	340	4.36
Pocatello Formation upper diamictite	NA	0.7	78	5.4	72.6	11.6	0.76	0.88	3.48	65	120	300	3.89
Pocatello Formation upper diamictite	NA	0.7			72.4	11.9	0.46	1.07	3.43	67	122	325	3.64
Pocatello Formation lower diamictite	NA	0.7			63.8	14.8	0.74	1.48	4.3	67	189	678	3.96
Pocatello Formation lower diamictite	NA	0.7			66	13.4	0.62	1.43	3.89	66	152	532	3.24
Blaubeker Formation	AF	0.7	106	4	76.9	10	0.32	1.52	3.02	62	110	204	2.38
Blaubeker Formation	AF	0.7	86	4.7	75	9.85	1.42	2.13	2.83	53	92.7	243	1.67
Blaubeker Formation	AF	0.7	74	4.4	77.5	10.3	0.33	1.47	3.39	62	118	242	4.2
Kaigas Formation	AF	0.75	315	3.8	62.2	16.5	0.96	2.58	3.41	64	192	228	9.74
Kaigas Formation	AF	0.75	353	3.7	62.3	15.4	3.09	3.13	2.79	54	161	250	6.86
Kaigas Formation	AF	0.75	193	3.3	66.5	13.5	3.21	3.32	3.04	49	189	179	13
Numees Formation	AF	0.6	96	6.4	73.7	11.3	1.66	1.33	3.55	58	157	151	5.04
Numees Formation	AF	0.6	89	7.8	68.5	12.2	2.89	2.08	3.39	54			4.5
Numees Formation	AF	0.6	100	8.5	57.4	18.3	1.41	2.04	4.5	64			
Numees Formation	AF	0.6			71.1	13.2	1.32	2.21	3.33	59	174	237	6
Numees Formation	AF	0.6			70.6	14.5	0.39	2.17	4.92	61	231	188	3.85
Numees Formation	AF	0.6			70.8	14.6	0.31	2.3	5.14	61	232	219	5.28

Table S-1 Cont.

Stratigraphic unit	Continent	Age	N	$\delta^{15}N$	SiO_2	Al_2O_3	CaO	Na_2O	K_2O	CIA	Rb	Zr	Cs
Ghaub Formation	AF	0.64	163	-0.4	38.7	8.44	20.76	0.65	2.69	64	101	137	11.5
Ghaub Formation	AF	0.64	463	2.2	25	5.16	35.35	0.49	1.45	63	52.3	63.7	5.63
Ghaub Formation	AF	0.64	320	1.2	50	13.5	9.61	1.14	3.36	65	127	193	11.9
Chuos Formation	AF	0.7	306	2.8	42.2	7.77	14.03	0.71	2.84	60	136	125	9.27
Chuos Formation	AF	0.7	467	3	46.7	7.95	11.79	1.12	2.58	56	102	150	4.12
Chuos Formation	AF	0.7	397	2.5									
Gaskiers Formation	NA	0.58	83	1.3	65.5	15.5	1.07	2.89	4.46	58	113	203	8.28
Gaskiers Formation	NA	0.58	109	2.6	67.9	14	0.88	3.5	2.88	58	77.1	179	5.2
Gaskiers Formation	NA	0.58	103	2.1	64.9	15.8	1.64	4.59	2.5	55	65	205	4.44
Gaskiers Formation	NA	0.58			65.1	15.3	1.21	3.52	3.45	57	89.7	220	4.6704
Bolivia	SA	0.3	321	3.2	67.2	15.9	0.37	0.85	3.23	75	125	155	7.06
Bolivia	SA	0.3	357	2.6	65.1	16.2	0.49	1.13	3.6	72	146	232	9.47
Bolivia	SA	0.3	314	2.1	78.4	9.66	0.48	1.6	2.37	62	84.7	276	3.15
Bolivia	SA	0.3			77.2	11	0.21	1.02	2.7	70	106	257	5.21
Bolivia	SA	0.3			77.9	10.1	0.2	0.73	2.77	70	110	269	5.84
Bolivia	SA	0.3			78.1	9.52	0.78	1.24	2.25	63	85.3	252	3.72
DwykaEast Group	AF	0.3	373	2.1	41	9.86	10.25	1.13	1.81	66	66.7	109	3.62
DwykaEast Group	AF	0.3	461	3.3	54.9	12.4	3.31	1.63	2.31	61	82.3	135	4.35
DwykaEast Group	AF	0.3	386	2.8	53.6	12.4	3.52	1.58	2.32	62	86.5	147	4.3
DwykaEast Group	AF	0.3			53.9	13	1.79	0.95	3.28	66	136	127	8.64
DwykaEast Group	AF	0.3			29.8	5.73	16.47	0.46	1.1	69	45.1	59.5	2.47
DwykaEast Group	AF	0.3			27.9	4.52	18.89	0.49	0.91	64	31.4	73.3	1.63
DwykaEast Group	AF	0.3			38	6.43	17.66	0.65	1.15	67	40.4	74.3	1.6
DwykaEast Group	AF	0.3			45.1	7.17	9.74	0.31	1.1	78	33.2	85.7	1.08
DwykaWest	AF	0.3	340	8	63.9	15	1.69	3.06	3.27	57	125	201	2.12
DwykaWest	AF	0.3	372	8	75.3	10.6	0.8	3.19	2.18	55			
DwykaWest	AF	0.3	332	8	69.4	12.6	1.22	3.15	2.41	56	80.9	232	1.28
DwykaWest	AF	0.3			65.8	14.6	2.07	3.07	3.26	55	114	204	2.97
DwykaWest	AF	0.3			67	14.2	1.99	2.97	3.19	55			
DwykaWest	AF	0.3			64.7	15.1	1.93	2.95	3.44	57	135	227	6.72
DwykaWest	AF	0.3			68.8	13.5	1.26	3.57	2.77	56	95.9	245	1.69
DwykaWest	AF	0.3			67	6.38	10.51	1.61	0.99	50			
Till4	NA	0.001	440	4.3	65	14.4	1.25	3.04	3.25	66	161	385	12

Constraining Post-depositional Alteration

Crucial to our presented interpretation is demonstrating that the N concentrations have not been altered through time. That is, the lower concentrations observed in older rocks are not simply the result of progressive N loss through time. There are a number of approaches to assess this possibility. Firstly, we observe no correlation between $\delta^{15}N$ values and N concentration (Fig. S-1). If progressive N loss was occurring, the expected trend would be higher $\delta^{15}N$ values associated with lower N concentrations, due to the preferential loss of ^{14}N during diagenesis.

Secondly, comparisons with other elemental compositions indicate lack of alteration through time. As discussed in detail in Gaschnig *et al.* (2016), a first-pass approach is to use the Chemical Index of Alteration (CIA), which is defined as: Al_2O_3 / (Al_2O_3 + CaO* + Na_2O + K_2O) × 100 (Nesbitt and Young, 1982). This index supposes that alteration of feldspars to clay minerals during chemical alteration and weathering will increase the CIA. There is no observed correlation between N concentration and CIA in these samples (Fig. S-2). As discussed in Gaschnig *et al.* (2016), till samples with a high CIA likely inherited this signal from a weathered source rock, rather than having experienced extensive chemical weathering themselves.

An additional comparison can be made using Large Ion Lithophile (LILE) and High Field Strength Elements (HFSE). Both these groups are incompatible, but in general LILE are fluid-mobile and HFSE are not. We use Cs to represent LILE and Zr to represent HFSE. Neither Zr nor Cs abundances in the crust have shown secular changes through time (Gaschnig *et al.*, 2016). If progressive N loss *via* aqueous alteration through time was the sole cause for the trend in increased N through time, samples that have low N would have a correspondingly low Cs/Zr. While samples with the very lowest N and Cs/Zr are from the Archean/Palaeoproterozoic (Fig. S-3), there are also a number of younger samples with low Cs/Zr and high N. Thus, we suggest that post-depositional aqueous alteration alone cannot explain the trend of decreased N concentrations back in time, though we cannot rule out some alteration for the lowest N samples.

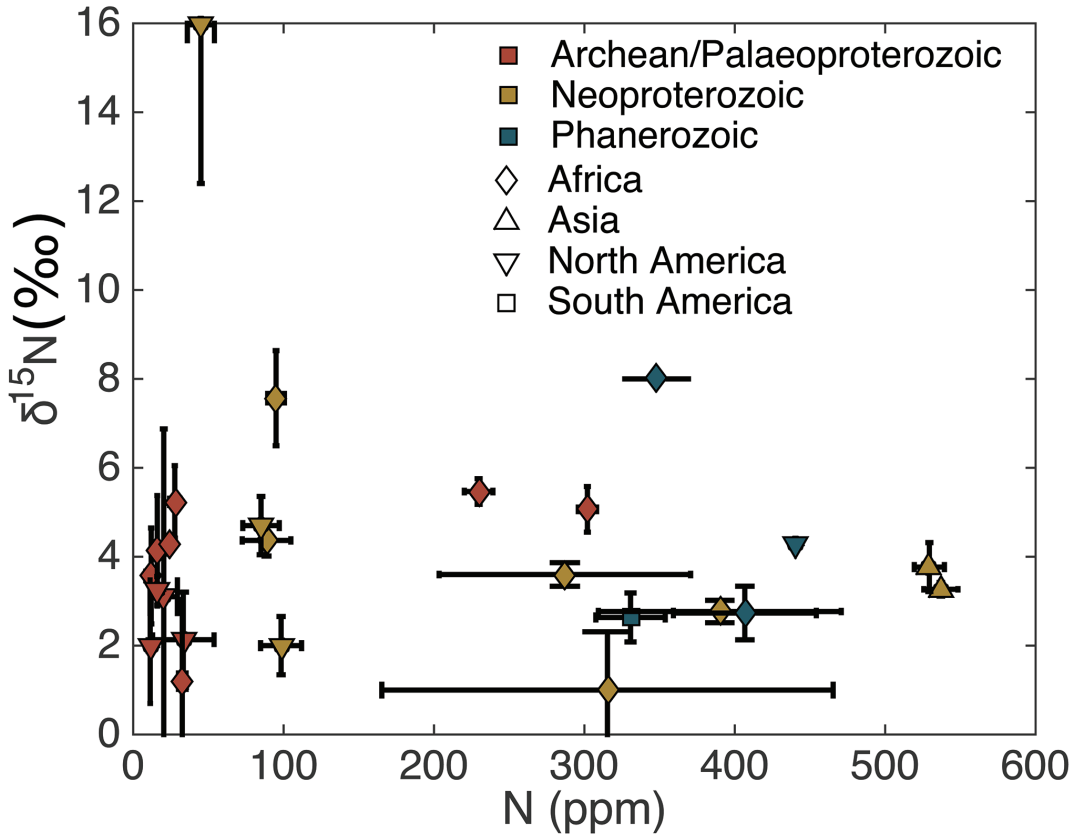

Figure S-1 Nitrogen isotope values plotted against N concentration. Lack of correlation between isotopes and concentrations from samples of all ages suggests that there has not been N loss during diagenesis. Nitrogen loss tends to result in samples with low N concentration having high $\delta^{15}N$ values, which is not observed.

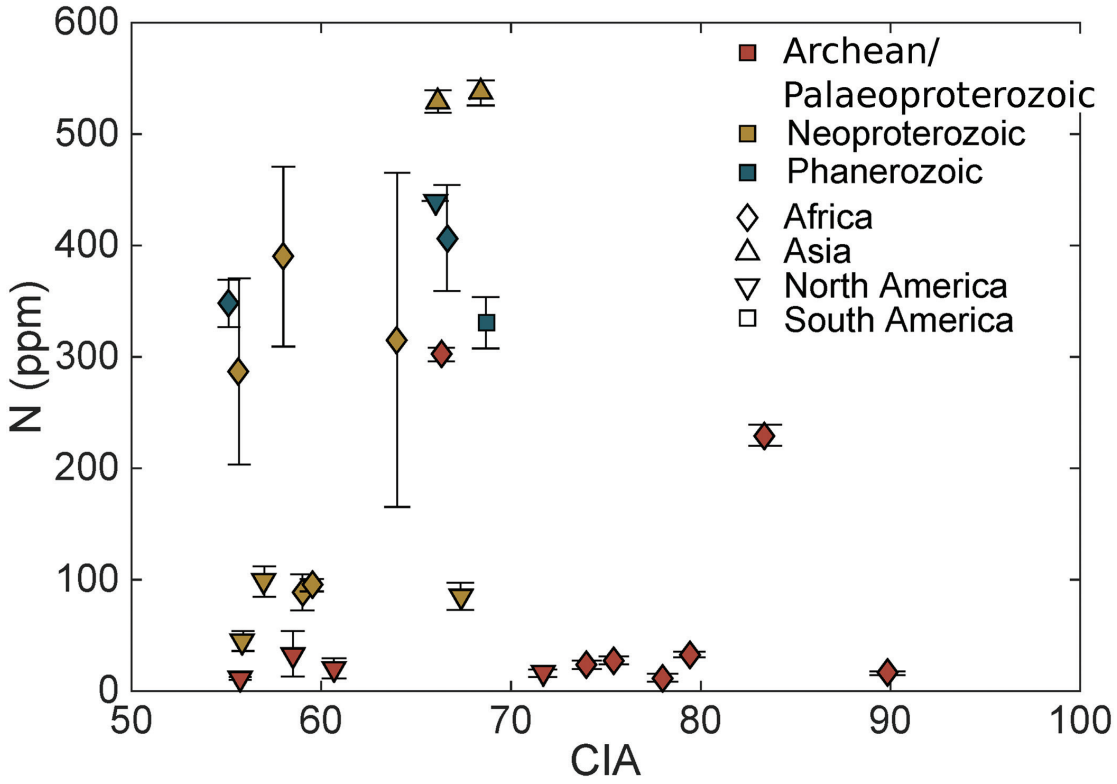

Figure S-2 Nitrogen concentration plotted against Chemical Index of Alteration (CIA). See text for details, but lack of correlation suggests that aqueous alteration alone cannot explain the increase in N concentration through time.

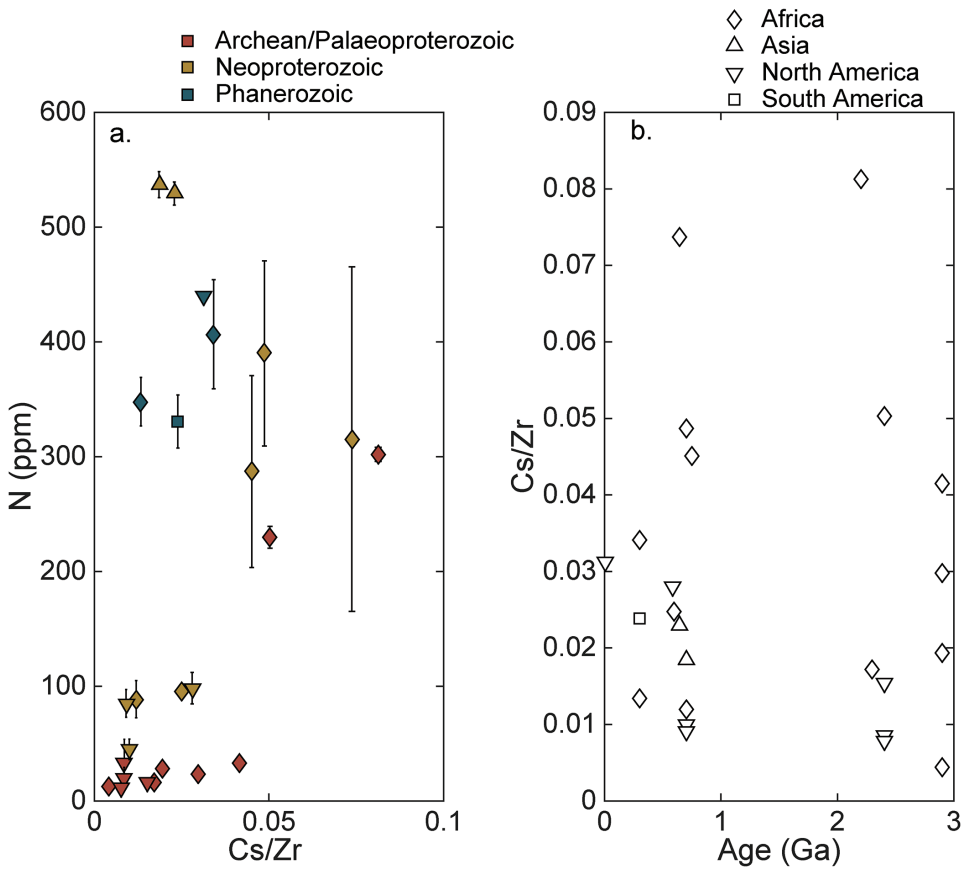

Figure S-3 Nitrogen concentration plotted against Cs/Zr. See text for details, but lack of correlation suggests that aqueous alteration alone cannot explain the increase in N concentration through time, with the possible exception of the lowest N samples. There is no change in the Cs/Zr ratio through time, suggesting that geographic and temporal evolution of Cs and Zr does not explain variation seen.

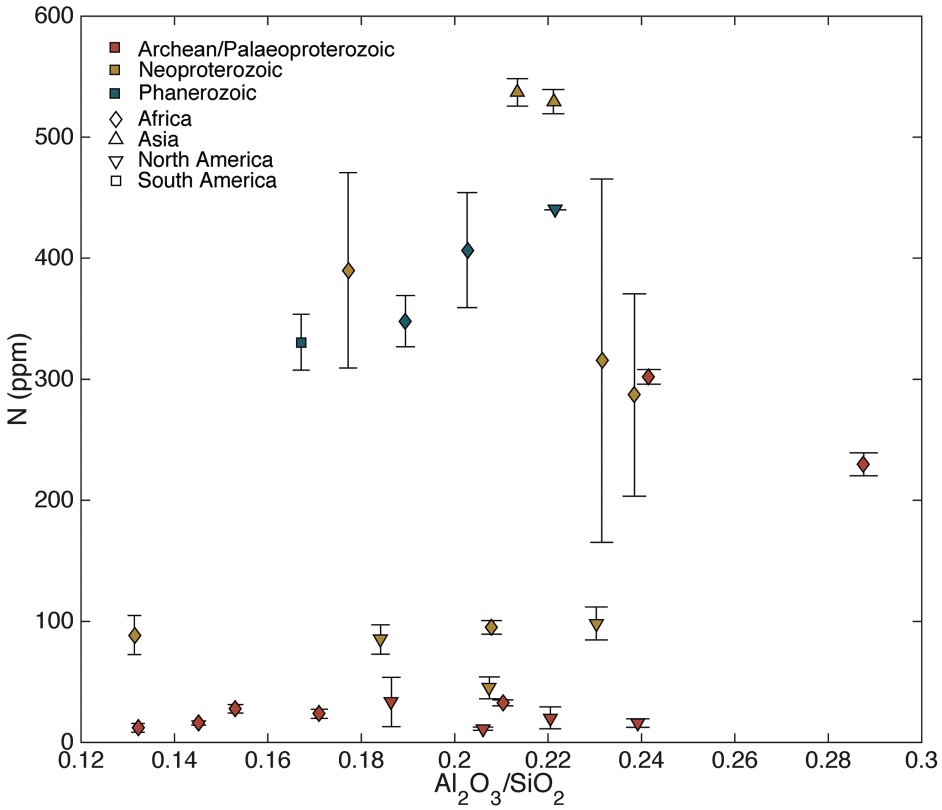

Figure S-4 Nitrogen concentration plotted against Al_2O_3/SiO_2.

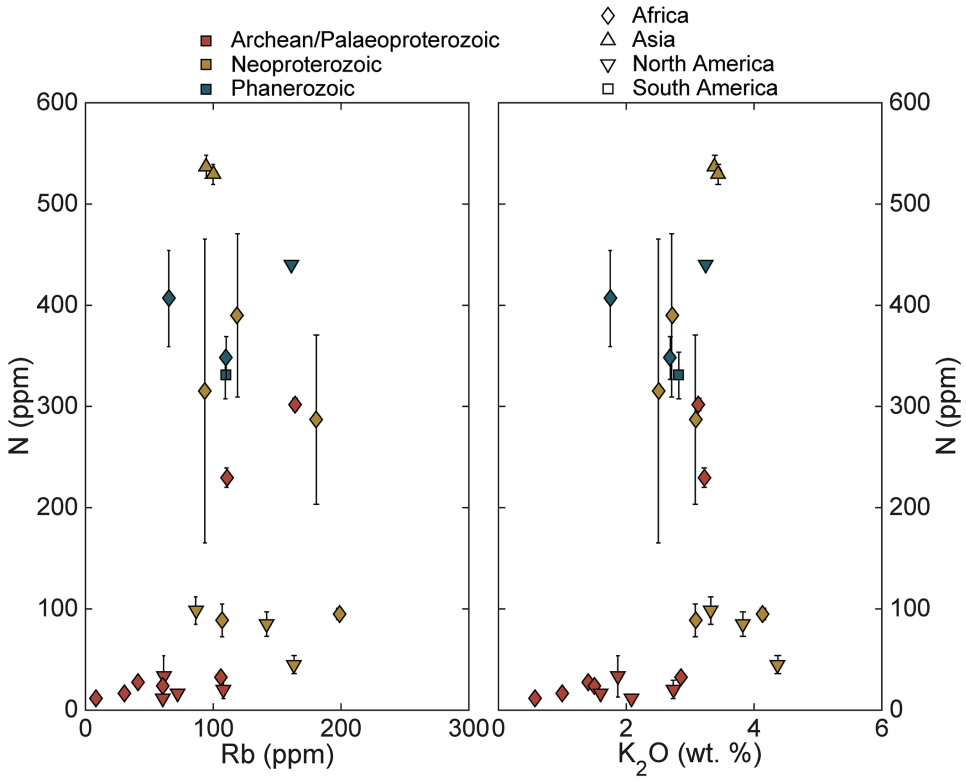

Figure S-5 Nitrogen concentration plotted against Rb and K_2O. We note that for low N samples there is a positive correlation, but for moderate and high N samples, no correlation is observed.

Mineral Hosts for Nitrogen

We do not know the exact mineral host of N in these samples. Typically, NH_4^+ is the most common geological species of N, though there may be small amounts of organic N as well. In detail, some samples that have high N also have a high Al_2O_3/SiO_2 ratio (Fig. S-4), which is indicative of a weathering environment rich in feldspars and clays compared to quartz (Gaschnig *et al.*, 2016, and references therein). Thus, for many samples, K-bearing phases are a likely host for N as NH_4^+, though the lack of correlation between N and Rb (which also substitutes for K), indicates that this simple relationship may not be true for all samples (Fig. S-5).

Palaeoproterozoic samples from South Africa exemplify this relationship (Fig. S-4). Other high N samples, such as those from North America, have a similar Al_2O_3/SiO_2 ratio as higher N samples from Africa and South America, indicating clays/feldspars may not be the main host for N. Another mineral may be the host in these settings.

Nitrogen Concentrations by Continent

As mentioned in the main text, there is an apparent relationship between the current continent of each sample and N concentration. That is, samples from Africa, South America, and Asia are generally high while samples from North American are generally low. The strongest correlation both regionally and globally is age, but another possibility that could explain some of the geographic control is a different history of continental growth and assemblage. Zircon ages from Africa and North America from the compilation of Belousova *et al.* (2010) show two peaks and one peak in ages, respectively (Fig. S-6).

If these zircon age peaks correspond with periods of enhanced continental growth, it would suggest that Africa grew somewhat earlier than North America, and correspondingly biologically processed N was incorporated during this phase of continental growth. A major continental growth period occurred later in North America, around 1.2 Ga, with an increase in N in till samples not seen until the Phanerozoic. There would be some lag time between continental growth and erosion by glaciers, thus these periods of growth represent a maximum hypothesised age of N incorporation for each continent. A reasonable test of this pulsed N addition hypothesis would be the analysis of N concentration in felsic intrusive igneous rocks, which are more temporally associated with the continental-growth phases. Though there are few till samples from Asia and South America, distinct zircon age peak distributions indicate possible different continental growth histories, with correspondingly distinct N histories.

It is also possible that palaeogeography could exert a control over timing of N incorporation. However, if the source of N to the continental crust is biologically processed, subduction zone transported material, both the manner of biologic processing and geometry and extent of subduction zones should have a greater effect. Perhaps, though, if continental subduction zones are located nearer to more productive areas, more N could be buried with organic matter and processed in a subduction zone. Indeed, areas with high productivity near Central America have more N in sediments than low-productivity areas in the eastern Pacific (Elkins *et al.*, 2006; Mitchell *et al.*, 2010).

In the modern ocean, areas with high levels of N-fixing (driving atmospheric N_2 drawdown) are mostly identified in the tropics. Thus, it is possible that high N-fixing or high productivity areas overlying subduction zones could enhance incorporation of N into continental crust. The distribution of N-fixing regions throughout geologic time are poorly constrained; we are not aware of any data speaking to this directly. In addition, the temperature/pH/redox of subduction zones seems to exert strong control over the fate of subducted N (Busigny *et al.*, 2011; Mikhail and Sverjensky, 2014), and might be more important than palaeogeography.

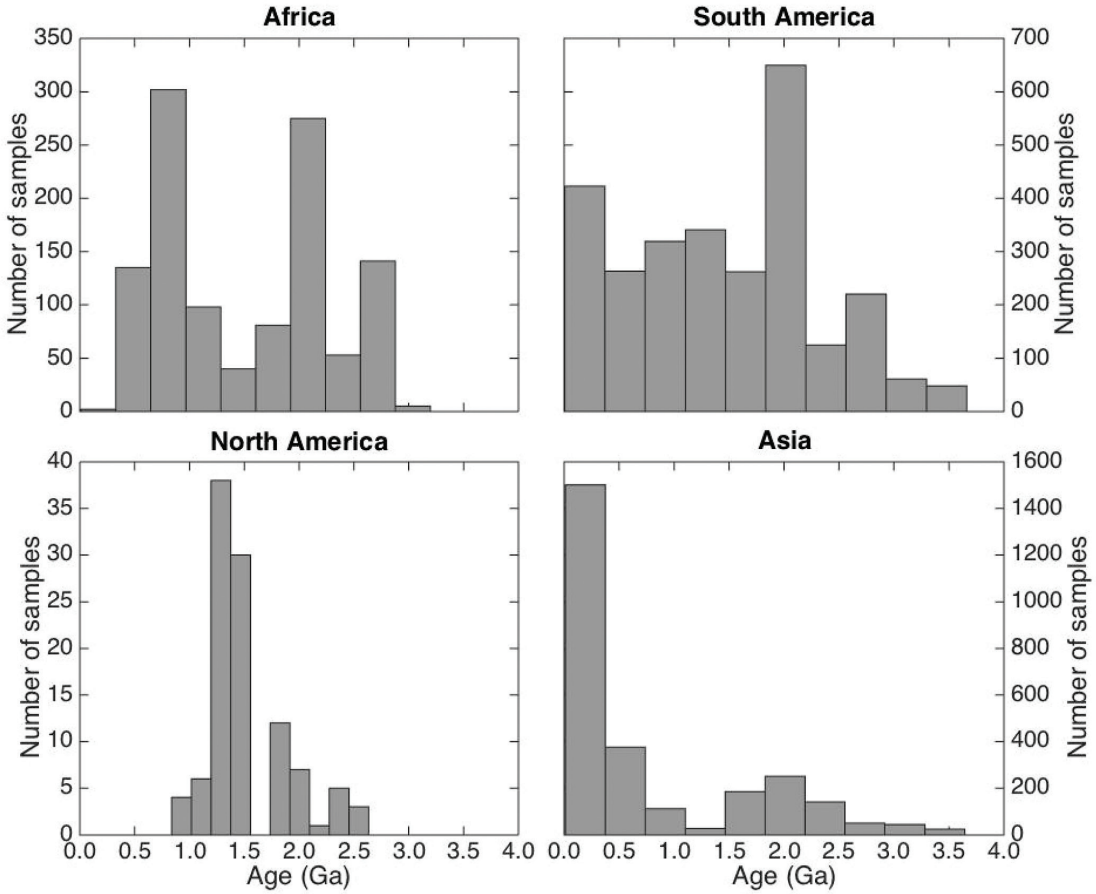

Figure S-6 Histograms of detrital zircons from Africa, South America, North America, and Asia through time. African zircons have two peaks at 2.1 and 0.75 Ga, while South America has the peak at 2.1 Ga, and perhaps a peak from 0 to 0.5 Ga. Both North America and Asia have a single dominant peak, at 1.2 Ga and 0–0.5 Ga, respectively. It is possible that peaks in ages correspond to periods of continental growth and, by extension, periods of N-sequestration in the crust.

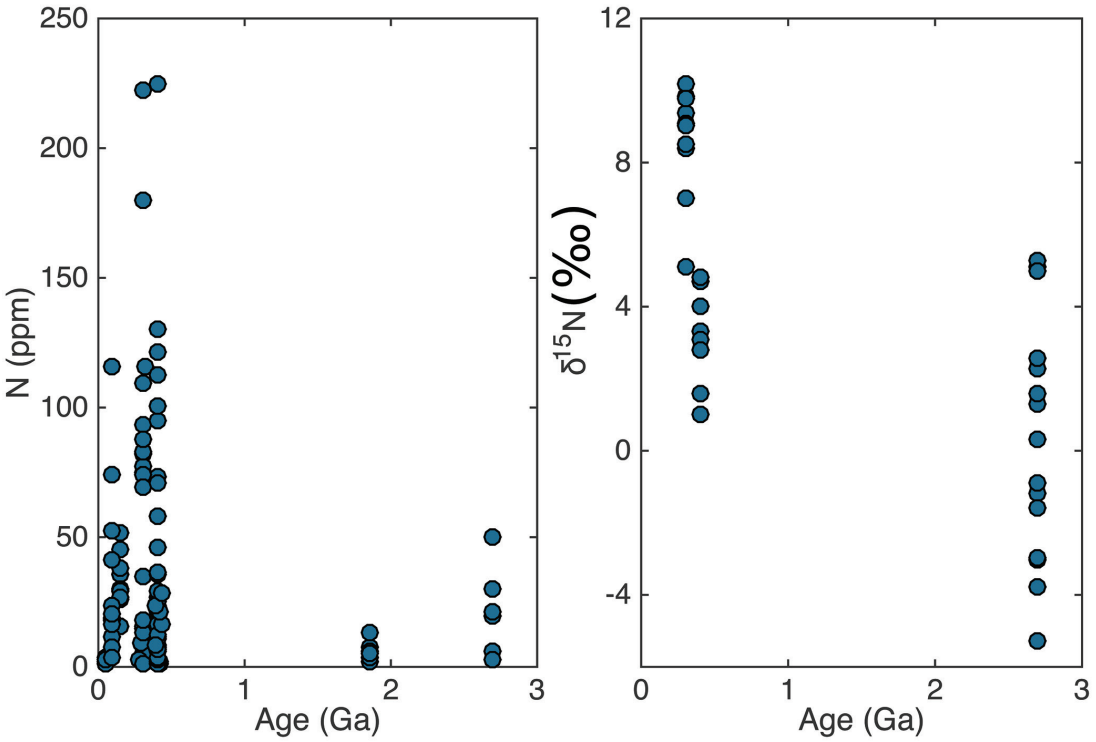

Figure S-7 Nitrogen concentration and $\delta^{15}N$ values of granitic rocks through time. These data are consistent with an increase in N content of continental crust through time, with increase in isotopic values consistent with a biologically processed source for said N.

Granitic Nitrogen

Nitrogen concentration and isotopic data from the compilation of Johnson and Goldblatt (2015) are shown in Figure S-7. These are data from both whole rock and mineral specific N analyses, scaled up to whole rock values. The rocks analysed are from the British Isles (Hall, 1987, 1988, 1993; Cooper and Bradley, 1990; Bebout *et al*., 1999), southern Europe (Hall *et al*., 1991; Hall, 1999), the Canadian shield (Jia and Kerrich, 2000), Iran (Ahadnejad *et al*., 2011), Finland (Itihara and Suwa, 1985), and the United States (Hoering, 1955). While data are sparse, especially isotopic data, they are consistent with an increase in crustal N through time. Samples from the Archean and Palaeoproterozoic have a mean N concentration of 16 ppm, while those from the Phanerozoic average 43 ppm N. These means are statistically different as shown by Student's t-test (Student, 1908). Isotopic data may increase from depleted, mantle-like values towards more enriched, biologic/sedimentary values through time. Analyses are heavily biased towards Europe, and especially the British Isles. Additional geographic coverage, in addition to temporal coverage, would greatly help with future interpretations.

Supplementary Information References

Ahadnejad, V., Hirt, A.M., Valizadeh, M.-V., Bokani, S.J. (2011) The ammonium content in the Malayer igneous and metamorphic rocks (Sanandaj-Sirjan Zone, Western Iran). *Geologica Carpathica* 62, 171–180.

Bebout, G., Cooper, D., Bradley, A.D., Sadofsky, S.J. (1999) Nitrogen-isotope record of fluid- rock interactions in the Skiddaw Auerole and granite, English Lake District. *American Mineralogist* 84, 1495–1505.

Belousova, E., Kostitsyn, Y., Griffin, W.L., Begg, G.C., O'Reilly, S.Y., Pearson, N.J. (2010) The growth of the continental crust: constraints from zircon Hf-isotope data. *Lithos* 119, 457–466.

Busigny, V., Cartigny, P., Philippot, P. (2011) Nitrogen isotopes in ophiolitic metagabbros: A re-evaluation of modern nitrogen fluxes in subduction zones and implication for the early earth atmosphere. *Geochimica et Cosmochimica Acta* 75, 7502–7521.

Cooper, D., Bradley, A. (1990) The ammonium content of granites in the English Lake District. *Geological Magazine* 127, 579–586.

Elkins, L., Fischer, T., Hilton, D., Sharp, Z., McKnight, S., Walker, J. (2006) Tracing nitrogen in volcanic and geothermal volatiles from the Nicaraguan volcanic front. *Geochimica et Cosmochimica Acta* 70, 5215–5235.

Gaschnig, R.M., Rudnick, R.L., McDonough, W.F., Kaufman, A.J., Valley, J.W., Hu, Z., Gao, S., Beck, M.L. (2016) Compositional evolution of the upper continental crust through time, as constrained by ancient glacial diamictites. *Geochimica et Cosmochimica Acta* 186, 316–343.

Hall, A. (1987) The ammonium content of Caledonian granites. *Journal of the Geological Society* 144, 671–674.

Hall, A. (1988) The distribution of ammonium in granites from South-West England. *Journal of the Geological Society* 145, 37–41.

Hall, A. (1993) Application of the indophenol blue method to the determination of ammonium in silicate rocks and minerals. *Applied Geochemistry* 8, 101–105.

Hall, A. (1999) Ammonium in granites and its petrogenetic significance. *Earth-Science Reviews* 45, 145–165.

Hall, A., Bencini, A., Poli, G. (1991) Magmatic and hydrothermal ammonium in granites of the Tuscan magmatic province, Italy. *Geochimica et Cosmochimica Acta* 55, 3657–3664.

Hoering, T. (1955) Variations of nitrogen-15 abundance in naturally occurring substances. *Science* 122, 1233–1234.

Itihara, Y., Suwa, K. (1985) Ammonium contents of biotites from Precambrian rocks in Finland: The significance of NH_4^+ as a possible chemical fossil. *Geochimica et Cosmochimica Acta* 49, 145–151.

Jia, Y., Kerrich, R. (2000) Giant quartz vein systems in accretionary orogenic belts: the evidence for a metamorphic fluid origin from $\delta^{15}N$ - $\delta^{13}C$ studies. *Earth and Planetary Science Letters* 184, 211–224.

Johnson, B.W., Goldblatt, C. (2015) The Nitrogen Budget of Earth. *Earth Science Reviews* 148, 150–173.

Mikhail, S., Sverjensky, D.A. (2014) Nitrogen speciation in upper mantle fluids and the origin of Earth's nitrogen-rich atmosphere. *Nature Geoscience* 7, 816–819.

Mitchell, E.C., Fischer, T.P., Hilton, D.R., Hauri, E.H., Shaw, A.M., de Moor, J.M., Sharp, Z.D., Kazahaya, K. (2010) Nitrogen sources and recycling at subduction zones: Insights from the Izu-Bonin-Mariana arc. *Geochemistry, Geophysics, Geosystems* 11, Q02X11, doi:10.1029/2009GC002783.

Nesbitt, H., Young, G. (1982) Early Proterozoic climates and plate motions inferred from major element chemistry of lutites. *Nature* 299, 715–717.

Student (1908) The probable error of a mean. *Biometrika* 6, 1–25.

Stüeken, E.E. (2013) A test of the nitrogen-limitation hypothesis for retarded eukaryote radiation: nitrogen isotopes across a Mesoproterozoic basinal profile. *Geochimica et Cosmochimica Acta* 120, 121–139.